How a Protein Binds B_{12}: A 3.0 Å X-ray Structure of B_{12}-Binding Domains of Methionine Synthase

Catherine Luschinsky Drennan, Sha Huang, James T. Drummond, Rowena G. Matthews, Martha L. Ludwig*

The crystal structure of a 27-kilodalton methylcobalamin-containing fragment of methionine synthase from *Escherichia coli* was determined at 3.0 Å resolution. This structure depicts cobalamin-protein interactions and reveals that the corrin macrocycle lies between a helical amino-terminal domain and an α/β carboxyl-terminal domain that is a variant of the Rossmann fold. Methylcobalamin undergoes a conformational change on binding the protein; the dimethylbenzimidazole group, which is coordinated to the cobalt in the free cofactor, moves away from the corrin and is replaced by a histidine contributed by the protein. The sequence Asp-X-His-X-X-Gly, which contains this histidine ligand, is conserved in the adenosylcobalamin-dependent enzymes methylmalonyl–coenzyme A mutase and glutamate mutase, suggesting that displacement of the dimethylbenzimidazole will be a feature common to many cobalamin-binding proteins. Thus the cobalt ligand, His^{759}, and the neighboring residues Asp^{757} and Ser^{810}, may form a catalytic quartet, Co-His-Asp-Ser, that modulates the reactivity of the B_{12} prosthetic group in methionine synthase.

Derivatives of vitamin B_{12} or cobalamin serve as the prosthetic groups for the two enzymes methionine synthase and methylmalonyl-CoA mutase, found in both humans and prokaryotes, and for several other enzymes found in prokaryotes. The prokaryotic enzymes include adenosylcobalamin-dependent ribonucleotide reductase, glutamate mutase, ethanolamine ammonialyase, various aminomutases, and propanediol dehydrase (*1*). Cobalamin-dependent enzymes catalyze some of the more difficult reactions known, such as carbon skeleton rearrangements or the removal of a methyl group from a tertiary amine. These reactions exploit the ability of the cobalamin prosthetic group to form a carbon-cobalt bond, linking cobalt to a methyl group in methylcobalamin (Fig. 1), to a cyano group in cyanocobalamin, or to the 5′ position of 5′-deoxyadenosine in adenosylcobalamin (coenzyme B_{12}). Those enzymes that bind adenosylcobalamin catalyze group migrations by mechanisms that are typically initiated by homolytic cleavage of the carbon-cobalt bond of the cofactor to form an adenosyl radical and cob(II)alamin. In contrast, enzymes that use methylcobalamin as the cofactor catalyze methyl transfer reactions. These reactions formally proceed by heterolytic cleavage of the carbon-cobalt bond of the cofactor to form cob(I)alamin, with the methyl carbocation being transferred to the acceptor substrate. The overall reaction catalyzed by methionine synthase involves two successive methyl transfers:

$$CH_3\text{-cob(III)alamin} + \text{homocysteine} \rightarrow \text{cob(I)alamin} + \text{methionine} \quad (1)$$

$$\text{Cob(I)alamin} + \text{methyltetrahydrofolate} \rightarrow CH_3\text{-cob(III)alamin} + \text{tetrahydrofolate} \quad (2)$$

A central issue is how the reactivity of cobalamin is controlled to favor heterolytic cleavage of the carbon-cobalt bond in one class of enzymes and homolytic cleavage in the other. Model studies have emphasized the importance of the lower axial ligand in determining the strength and mode of cleavage of the bond between cobalt and an alkyl ligand in the upper axial position (*2–4*).

The cobalamin prosthetic group is the largest and most complicated of the organic cofactors. The structure of cyanocobalamin (vitamin B_{12}) was determined by x-ray crystallography more than 30 years ago (*5*), and the crystal structures of adenosylcobalamin and methylcobalamin are also known (*6, 7*). The presence of the heme-like corrin and the dimethylbenzimidazole nucleotide moiety in cobalamin has prompted speculation that B_{12}-dependent enzymes might incorporate globin- or nucleotide-binding folds, but these enzymes show little or no sequence similarity or identity with proteins that bind hemes or nucleotides. There is also little sequence similarity within the B_{12}-dependent enzyme family; such similarities among cobalamin-dependent enzymes have only recently been detected by Marsh and Holloway (*8*), who identified two short sequences that might be fingerprints for cobalamin-binding sites.

Methionine synthase from *Escherichia coli* is a large monomeric protein (136 kD, 1227 amino acid residues), composed of two functionally distinct regions. The NH_2-terminal 98-kD fragment, which includes a cobalamin-binding region at its COOH-terminus, catalyzes the transfer of the methyl group of methyltetrahydrofolate (CH_3-H_4folate) to homocysteine (Hcy) (*9*). The COOH-terminal 38-kD region participates in reductive activation of the enzyme. The cob(I)alamin intermediate is highly reactive and is occasionally oxidized to an inactive cob(II)alamin species. The enzyme must then be reactivated by reductive methylation to form methylcobalamin, which requires *S*-adenosyl-methionine (AdoMet) and an electron that is believed to be donated in vivo by flavodoxin (*10*). The cobalamin-binding region of the protein was initially isolated by digestion of the native enzyme with trypsin (*11*), and more

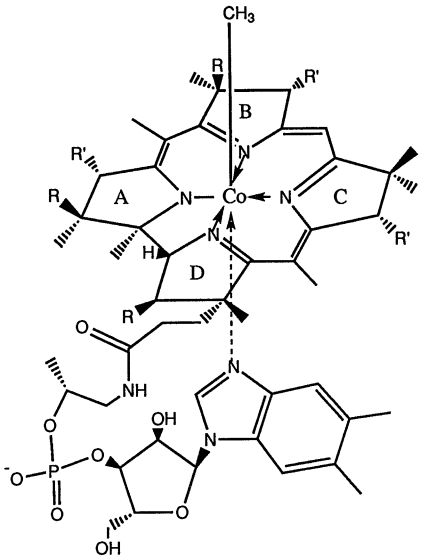

R = CH_2CONH_2

R' = $CH_2CH_2CONH_2$

Fig. 1. Chemical structure of methylcobalamin. Methylcobalamin contains the nucleotide base dimethylbenzimidazole, which is connected to the D ring of the corrin by a side chain that includes an unusual α sugar–nucleotide linkage and a ribose phosphorylated on the 3′, rather than the 5′, position. The corrin macrocycle is less symmetric than porphyrin, and is decorated with methyl, acetamide, and propionamide substituents. The central cobalt is hexacoordinate, with four nitrogen ligands provided by the corrin macrocycle, a methyl group in the upper (β) axial position, and a nitrogen (N3) from dimethylbenzimidazole in the lower (α) axial position.

C. L. Drennan, S. Huang, R. G. Matthews, and M. L. Ludwig are in the Biophysics Research Division and the Department of Biological Chemistry, University of Michigan, Ann Arbor, MI 48109–1055, USA. J. T. Drummond is now at the Department of Biochemistry, Duke University, Durham, NC 27710, USA.

*To whom correspondence should be addressed.

recently a 27-kD fragment extending from amino acids 651 to 896 has been crystallized (*12*). This fragment lacks the ability to catalyze methyl transfer reactions, but retains bound methylcobalamin. It is the structure of this fragment, which affords a first look at the three-dimensional interactions responsible for binding the cobalamin cofactor, that we now describe.

Table 1. Data collection and structure determination. Crystals of the 27-kD cobalamin-binding fragment (space group $P2_12_12_1$, a = 96.7, b = 55.3, c = 103.8 Å) were grown in PEG-6000, 50 mM tris, pH 7.5, at 20°C, starting from solutions of intact (M_r = 136,100) cobalamin-dependent methionine synthase from *E. coli*. Intensities were measured at 4°C with a dual area detector (San Diego Multiwire Systems). Heavy-atom parameters were refined with HEAVY (*26*) and then MLPHARE (*27*) to give an overall figure of merit from 30.0 to 4.0 Å of 0.46 for acentric reflections and 0.69 for centric reflections.

Parameter	Native	$NaAuCl_4$ (1 mM) (47 hours)	K_2PtCl_4 (3.2 mM) (48 hours)	$(CH_3)_3PbAc$ (15 mM) (2 weeks)	$SmAc_3$ (10 mM) (42 hours)
Resolution (d_{min}, Å)	3.0	3.3	3.3	3.1	3.8
Unique reflections (no.)	10417	8249	6678	9288	5557
Completeness (%)	89	93	77	88	96
Redundancy	3.1	2.4	3.0	2.6	2.7
I/σ(I) at d_{min}	2.0	2.0	2.2	2.1	1.9
R_{sym}	0.054	0.055	0.073	0.071	0.078
*$\langle F_h \rangle$rms/E		0.8	1.0	1.2	0.5

*Phasing power; E, closure error.

Table 2. Model building and refinement. The local twofold symmetry was determined initially by visual comparisons and from heavy atom sites, and was confirmed by means of density correlation in PROTEIN (*28*). The symmetry operation was refined in real space (*13*) to give a map correlation coefficient of 0.36. A cyclic procedure of model building followed by mask generation and averaging in PHASES (*29*) was then pursued until 3477 of the 3996 atoms of the cofactor and residues 651 to 896 had been positioned in 3.5 Å maps (stage 1). In stage 2 (*30*), phases were extended to 3.0 Å and the model was improved by cycling between refinement in X-PLOR (*14*), phase combination (*31*), and model building (*15*). Omit maps were computed for successive segments of the structure in the final stage of refinement (stage 3). Five residues of the loop connecting domains I and II, 740 to 744, are disordered in the refined structure. The rms deviations of protein atoms from ideal geometry are bond lengths, 0.012 Å; bond angles, 1.8°; dihedral angles, 23.5°; and improper dihedral angles, 1.8°; the correlation coefficient for observed and calculated amplitudes is 0.896.

Stage	Resolution (Å)	Reflections (no.)	Atoms (no.)	R^*_{start}	R^*_{end}
1. Map averaging	30.0–3.5	6766	3477		
2. Refinement, phase combination, model building	8.0–3.0	9019*	3996	0.497	0.238
3. Omit maps, model building	8.0–3.0	9019*	3998	0.238	0.183

*Reflections with $F>2\sigma(F)$.

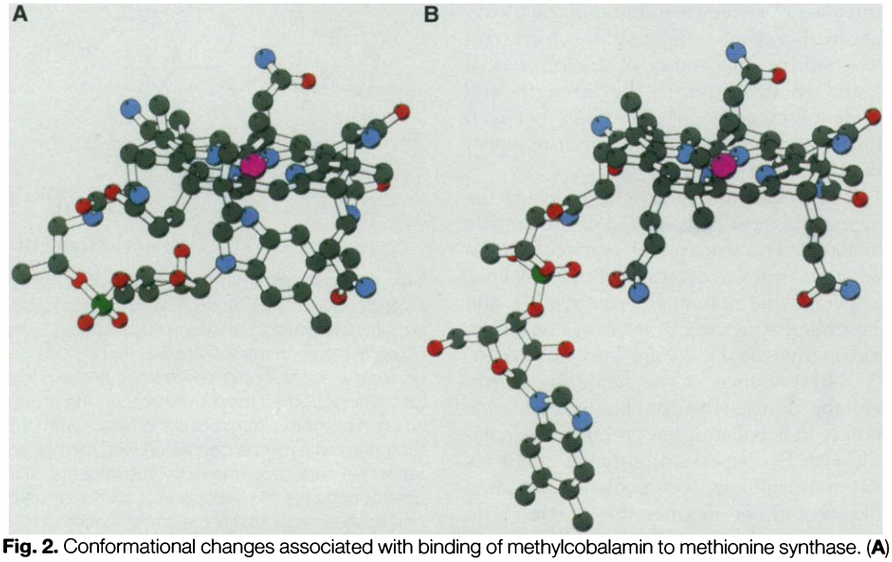

Fig. 2. Conformational changes associated with binding of methylcobalamin to methionine synthase. (**A**) The x-ray structure of free methylcobalamin (*7*) and (**B**) methylcobalamin bound to methionine synthase. Atom color-coding is as follows: C, dark gray; N, blue; O, red; P, green; and Co, magenta.

Structure determination and description. The structure was initially determined to 3.5 Å by isomorphous replacement (Table 1) and averaging of the electron densities corresponding to two molecules in the asymmetric unit. The averaging, performed at first with no envelopes around the equivalent densities (*13*), was a crucial step in the development of the structure. Phasing was extended to 3.0 Å by cycling between refinement in X-PLOR (*14*) and model building (*15*) (Table 2). The R factor for data from 8.0 to 3.0 Å is 0.183 (3996 protein and cofactor atoms, two waters).

The most striking feature of this structure is the change in conformation of methylcobalamin when it binds to methionine synthase. The dimethylbenzimidazole nucleotide is displaced from the cobalt of the corrin, and is extended to form what we refer to as the nucleotide tail (Fig. 2). The corrin portion of the cobalamin cofactor is sandwiched between the two domains of the 27-kD fragment of methionine synthase (Fig. 3) and the nucleotide tail penetrates into a deep pocket formed by residues of the COOH-terminal domain.

The 90 residues at the NH_2-terminus of the fragment form a helical bundle comprising two pairs of antiparallel helices. Although the arrangement of the four helices is reminiscent of the core of the globin fold, the cobalamin lies outside the helix bundle whereas the heme prosthetic group is enclosed by the helices of the globin core. A single long loop connects the helix-bundle domain of methionine synthase to an α/β domain with a fold that resembles the Rossmann fold of nucleotide-binding proteins. This COOH-terminal α/β domain includes six helices and five parallel β-sheet strands arranged with the same sheet topology (Fig. 3C) found in flavodoxins (*16*). The corrin ring is positioned beyond the COOH-termini of the first and third β-sheet strands, with its lower face interacting with protruding loops that connect strand IIβ1 to helix IIα1 and strand IIβ3 to helix IIα3. In the classic nucleotide-binding folds, the nucleotide is also bound at the COOH-terminal end of the β sheet, but differences between the cobalamin and pyridine nucleotide-binding sites are so large that the cofactors hardly overlap when the backbones of the α/β domains are superimposed. The loop connecting strand IIβ1 to helix IIα1 (residues 754 to 760) differs in sequence, conformation, and function from the analogous regions of pyridine nucleotide-dependent dehydrogenases. It fills a site that binds adenine in the dehydrogenases and, instead of binding a nucleotide phosphate (*17*), contributes the His^{759} ligand to cobalt.

The helical domain: A methyl cap. A significant feature of the interaction of the helix-bundle domain with the top of the corrin is the shielding of the methyl ligand of cobalamin. The turn between helices Iα3 and Iα4 caps the top of the corrin, isolating the methyl group from solvent (Fig. 4). It is hard to see how the substrates can react with cobalamin; major movements of the upper domain would be required for in-line methyl transfers to or from the cobalt of cobalamin. There are only a few domain-domain hydrogen bonds, and the single connection between the helix-bundle domain and the COOH-terminal α/β domain could facilitate motions of the helical domain to allow access of substrates during catalysis. Alternatively, methyl transfers catalyzed by methionine synthase may proceed by single electron transfer mechanisms (*18*), which have less stringent geometric requirements than direct in-line displacement mechanisms, and may permit approach of the substrates from the periphery of the corrin.

The helical domain and the methyl cap may occur only in methionine synthases. The different upper faces of methyl- and adenosylcobalamin are likely to interact with different structural motifs in the two classes of B_{12} enzymes, and the sequence that contacts the upper face of methylcobalamin in methionine synthase has no detectable homologies with adenosylcobalamin-containing enzymes.

The α/β domain as a common cobalamin-binding motif. Residues of the α/β domain are involved in binding the lower face of the corrin, as well as the dimethylbenzimidazole tail. All of the sequence similarities among B_{12}-dependent enzymes are found in the region that corresponds to the α/β domain of methionine synthase. Sequence alignments based on the location of these B_{12}-binding residues allow us to propose sequence fingerprints for cobalamin binding (Fig. 5). Four of the seven conserved residues of the consensus sequence

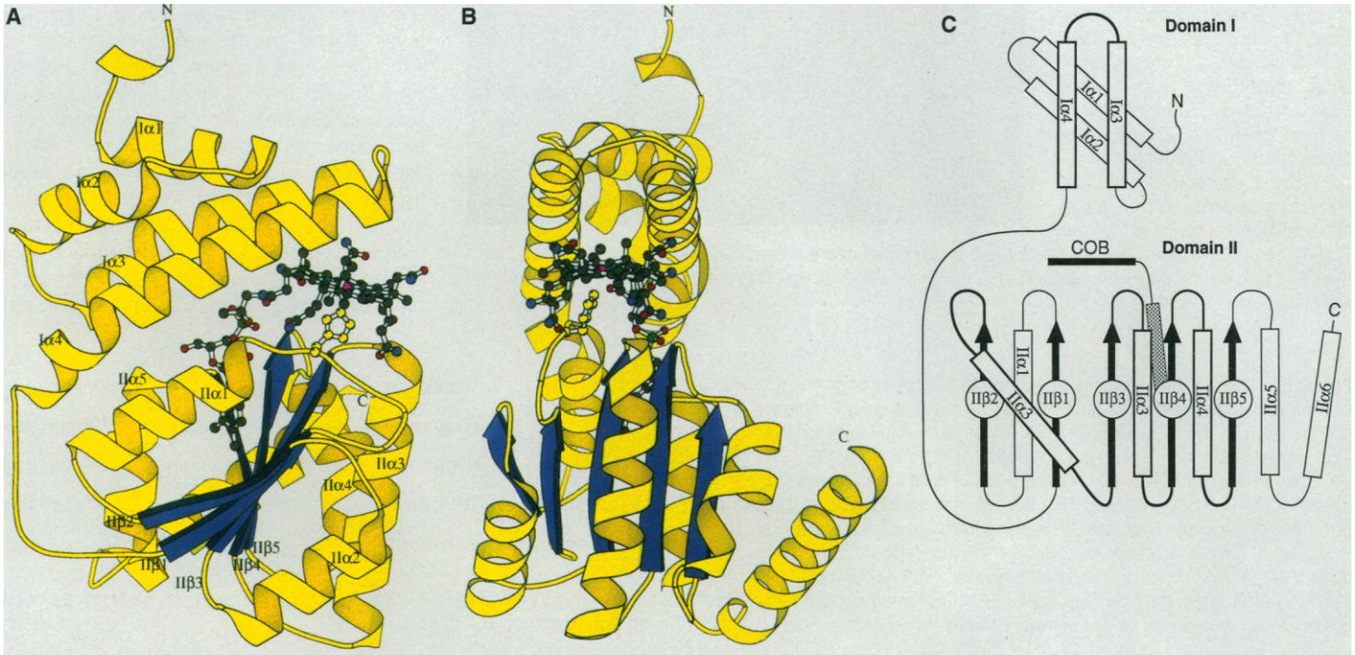

Fig. 3. The cobalamin-binding domains of methionine synthase. (**A**) A ribbon drawing with atoms of the cobalamin and His^{759} in ball-and-stick mode. The drawing was generated using MOLSCRIPT (*32*). The NH_2-terminal helical bundle domain is shown "above" the corrin. Kinks in helices Iα3 and Iα4, evident in the drawing, occur at prolines 696 and 734. (**B**) A ribbon drawing in an orientation rotated 90° from that shown in panel A. This orientation corresponds approximately to the topology diagram of panel C. In this view a striking feature is the narrow first domain, which is similar in width to the corrin macrocycle. In the intact enzyme, substrate-binding segments are expected to adjoin this domain. (**C**) Topology diagram. The helices of the first domain form a bundle according to the criteria of Harris *et al*. (*33*), with the front and back pairs of helices inclined at angles of 50° to 55°. In domain II, a doubly wound α/β fold, helices IIα1 and IIα5 are behind the sheet and IIα2, IIα3, and IIα4 are in front. Helix IIα6 makes substantial contacts with helix IIα5, but may also pack against other domains in intact methionine synthase. The corrin (COB) is indicated above the cleft between β-sheet strands 1 and 3; the dimethylbenzimidazole tail (shaded) adjoins strands β3 and β4 (Fig. 6). (**D**) Primary and secondary structure of the cobalamin-binding fragments of methionine synthase. The primary sequence of the cobalamin binding region of the *metH* gene from *E. coli* K-12 (EC) extending from residues 651 to 896 (*11*), and a homologous sequence including residues 621 to 867 of an open reading frame from *Mycobacterium leprae* (ML) (*34*) that is presumed to encode a cobalamin-dependent methionine synthase, are shown. These sequences have 27 percent identity overall, with conserved residues (boldface) concentrated in the cobalamin-binding regions. The secondary structural elements identified by hydrogen bonding patterns and the algorithm of Kabsch and Sander (*35*) are indicated below the sequences, and the regions assigned as fingerprints for both methyl- and adenosylcobalamin enzymes (Fig. 5) are marked with overhead bars.

D

```
          *   *   *   *   *   *   *   *
EC  651QAEWRSWEVN KRLEYSLVKG ITEFIEQDTE EARQQATRPI
ML  621EAELAKLPLF DRLAQRIVDG ERNGLDVDLD EAMTQ-KPPL
        <3>  <----Iα1---->    <----Iα2--->    <-

          *   *   *   *   *   *   *   *
EC  691EVIEGPLMDG MNVVGDLFGE GKMFLPQVVK SARVMKQAVA
ML  660AIINENLLDG MKTVGELFGS GQMQLPFVLQ SAEVMKAAVA
      ----------------Iα3--->    <------------Iα4---

          *   *       *   *   * _ _*  _  *   *
EC  731YLEPFIEASK EQ-GKTN--GKMV IATVKGDVHD IGKNIVGVVL
ML  700YLEPHMEKSD CDFGKGLAKGRIV LATVKGDVHD IGKNLVDIIL
      -------->             <-IIβ1->        <----IIα1-

          *   *   *   *   *   *   _*_   *
EC  771QCNN-YEIVDL GVMVPAEKIL RTAKEVNADL IGLSGLITPS
ML  743-SNNGYEVVNL GIKQPITNIL EVAEDKSADV VGMSGLLVKS
      -->    <IIβ2->   <----IIα2--->    <-IIβ3> <---

          *   *   *   *   __*   *   *   *
EC  811LDEMVNVAKE MERQGFT--IPL LIGGATTSKA HTAVKIEQNY
ML  783TVIMKENLEE MNTRGVAEKFPV LLGGAALTRS YVENDLAEVY
      ---IIα3-------->      <IIβ4>    <-IIα4-> <3>

          *   *   *   *   *   *   *   *   *
EC  851SGPTVYVQNA SRTVGVVAAL LSDTQRDDFV ARTRKEYETV RIQHGR
ML  825EGEVHYARDA FEGLKLMDTI MSAKRARRCA GEPGVLSCRS RPQ
      <IIβ5> <----IIα5---->   <--------IIα6------->
```

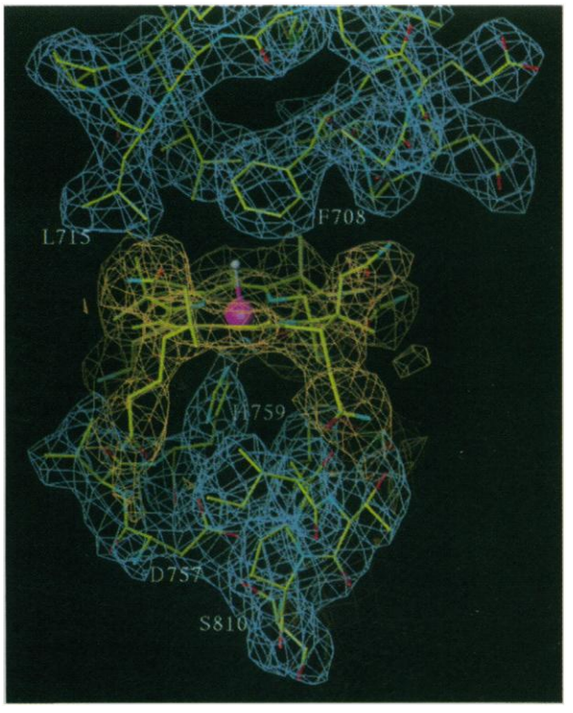

Fig. 4. View of electron density in the corrin binding site. The model resulting from refinement (Table 2) is displayed (*36*) in a map computed with coefficients ($2|F_o| - |F_c|$), including all data from 8.0 to 3.0 Å resolution. The contours around the cofactor are colored gold to distinguish density corresponding to methylcobalamin. Atom color coding is as follows: C, yellow; N, blue; O, red; S, green; and Co, magenta. The orientation is the same as that in Fig. 3B, with the edges of the A (right) and B (left) rings of the corrin at the front. Above the corrin are helices Iα3 and Iα4, viewed approximately along the helical axes, and connected by residues that contribute the "hydrophobic cap" over the corrin moiety. The side chain of Phe^{708} lies directly above the methyl group of methylcobalamin, protecting it from solvent. The acetamide side chains of corrin rings A and B, two of the characteristic substituents that occur in the B_{12} cofactor, are in positions to hydrogen bond to the protein backbone at residues 701 and 705 of the helical domain. Below the corrin are segments of the sequences that connect strain IIβ1 with helix IIα1 and strand IIβ3 with helix IIα3. His^{759}, the lower axial ligand to methylcobalamin, can be seen along with Asp^{757} and Ser^{810}.

(Fig. 5), Gly^{762}, Ser^{804}, and Gly^{833}-Gly^{834}, line the pocket that accommodates the nucleotide tail (Fig. 6). The first glycine is at the start of helix IIα1, where a side chain would make uncomfortably close contacts with the phosphate and sugar of the nucleotide tail. The last two glycines, Gly^{833} and Gly^{834}, also appear to be conserved for steric reasons. They are located at the COOH-terminus of strand IIβ4 where side chains would collide with dimethylbenzimidazole and ribose, respectively. The conserved Ser^{804} contributed by strand IIβ3 is in position to hydrogen bond to N3 of dimethylbenzimidazole, the same nitrogen that is coordinated to the cobalt in free methylcobalamin. Dimethylbenzimidazole is not involved in controlling the reactivity of the cobalamin because it is no longer the lower ligand to the cobalt. Instead, the structure of methionine synthase suggests that dimethylbenzimidazole is important for cofactor binding. Protein-cobalamin contacts bury approximately 715 of the 990 Å^2 accessible surface of the cofactor, and interactions between the extended nucleotide tail and the protein account for approximately 50 percent of the total surface area of methylcobalamin that is buried by contacts with the protein. The nucleotide tail

MS_Ec	^{757}DVHDIG	^{802}GLSGLITPS	^{829}PLLIGGA
MS_Ml	^{729}DVHDIG	^{775}GMSGLLVKS	^{803}PVLLGGA
MM_Hum	^{617}DGHDRG	^{662}GVSTLAAGH	^{690}LVMCGGV
GluM_Ct	^{14}DCHAVG	^{59}CVSSLYGQG	^{87}KLFVGGN
Consensus	DxHxxG--39/40--gxSxLxxxx-17/18-xxxxGGx		

Fig. 5. Structure-based sequence fingerprints. Residues conserved in the sequences of methionine synthase and adenosylcobalamin-dependent mutases (*8*) have been compared with the structure to derive fingerprint sequences for cobalamin binding. The sequences shown are those deduced for the cobalamin-dependent methionine synthase from *E. coli* [*MS_ec*] (*11*); the putative methionine synthase from *Mycobacterium leprae* (*34*) designated *MS_ml*; human methylmalonyl-CoA mutase [*MM_h*] (*37*); and the small subunit of glutamate mutase from *Clostridium tetanomorphum*, designated *GluM_Ct*, (*8*). Invariant residues are shown in bold. Three of the invariant residues, Asp^{757}, His^{759} (the cobalt ligand), and Leu^{806}, are contributed by the two loops that run under the corrin (see Figs. 4 and 8A). The remaining four invariant residues are involved in the binding of the nucleotide tail (see text). Invariant residues DxHxxG and the sequence GG were previously noted as significant motifs by Marsh and Holloway (*8*).

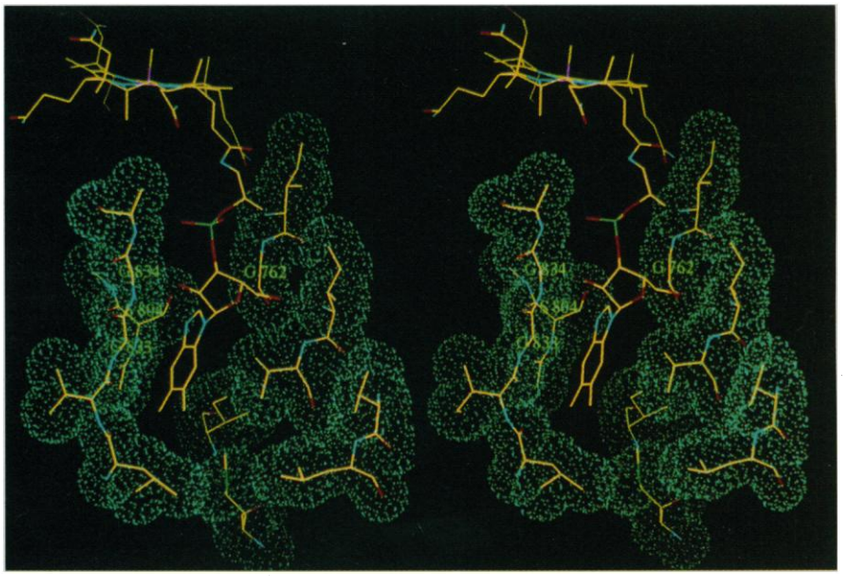

Fig. 6. A stereoview of the binding pocket that accommodates the dimethylbenzimidazole nucleotide. The remainder of methylcobalamin is shown for perspective. Atom color coding is as follows: C, yellow; N, blue; O, red; P, green; and S, green. Van der Waals surfaces have been drawn around portions of helix IIα1 and segments of sheet strands IIβ1, IIβ3, and IIβ4 to display the shape of the binding site. The "front wall" consisting of strand IIβ5 and helix IIα5 is not shown. Conserved residue Gly^{762} adjoins the phosphate-sugar binding site at the top of helix IIα1. The N3 of dimethylbenzimidazole interacts with Ser^{804} from Strand IIβ3, and the dimethylbenzimidazole nucleotide packs against the main chain at Gly^{833}-Gly^{834}, located at the top of strand IIβ4.

anchors the highly reactive cobalamin cofactor (Fig. 6).

The remaining three residues of the consensus sequence shown in Fig. 5, Asp^{757}, His^{759}, and Leu^{806}, are contributed by the loops that connect strand IIβ1 to helix IIα1 and strand IIβ3 to helix IIα3 (Fig. 4). The conserved histidine is the lower ligand to the cobalt in the structure of the 27-kD fragment of methionine synthase, Asp^{757} is in position to hydrogen bond with His^{759}, and Leu^{806} adjoins the histidine ligand. To confirm that methylcobalamin is also coordinated to a histidine residue in the intact protein, we used electron paramagnetic resonance spectroscopy (Fig. 7). This technique should be a useful probe for demonstrating the presence of histidine coordination to cobalt in other cobalamin-dependent enzymes. The conservation of the residues in the sequence motif shown in Fig. 5 suggests that the replacement of the dimethylbenzimidazole by a histidine ligand may be a common feature of cobalamin-binding to proteins.

A catalytic quartet in the reaction mechanism of B_{12}-dependent methionine synthase. The replacement of dimethylbenzimidazole with a histidine residue was unexpected and has profound implications for the catalytic mechanisms of B_{12}-dependent enzymes. As a result of this substitution, the control that the lower ligand exerts on the stability and reactivity of cobalamin derivatives is directly modulated by the protein rather than by a substituent of the cofactor. In the reaction catalyzed by methionine synthase, the protein must alternately stabilize methylcobalamin and cob(I)alamin species. In free cobalamins these forms are six and four coordinate, respectively (*19*). Model studies have demonstrated that the carbon cobalt bond is stabilized against homolytic cleavage to form cob(II)alamin (*2*) and against heterolytic cleavage to form cob(I)alamin (*3*) by basic lower ligands that increase the electron density on the cobalt. The ligand to cobalt in methionine synthase, His^{759}, is part of a hydrogen-bonded chain involving Asp^{757} and Ser^{810} that could provide a pathway for transfer of protons from solvent to the buried histidine (Fig. 8A). This feature of the structure prompts us to propose that protonation-deprotonation of the His-Asp pair might modulate the stability and reactivity of cobalamin in methionine synthase (*20*).

We suggest that, in the methylated form of the enzyme, Asp^{757} and His^{759} share a single proton, with one negative charge delocalized across the two residues. Ligation of His^{759} to methylcobalamin would favor formation of the proposed imidazolate species (*21*). Partial deprotonation of His^{759} would greatly increase the basicity of this ligand, stabilizing the methylated form of the enzyme. Reduction of enzyme-bound cob(II)alamin to cob(I)alamin has been shown to be associated with uptake of one proton (*22*), and we postulate that demethylation of methylcobalamin to form cob(I)alamin likewise involves protonation,

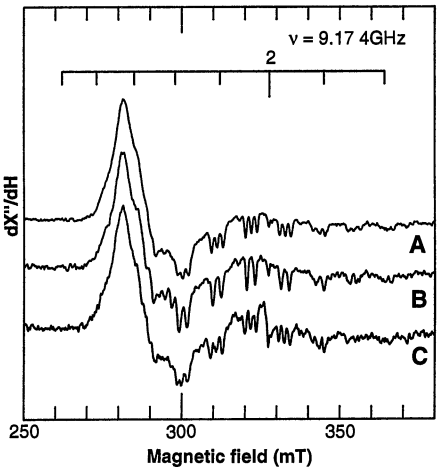

Fig. 7. Electron paramagnetic resonance (EPR) signals from cob(II)alamin in three different methionine synthase preparations (*38*). Curve A, enzyme was isolated from *E. coli* cells grown on glucose minimal MOPS medium containing $^{14}NH_4Cl$ and ^{14}N-labeled aquocobalamin. The interaction of the cobalt nucleus (spin = 7/2) with the unpaired electron in cob(II)alamin results in hyperfine splitting of the g_z signal into an octet centered at $g = 2$ (330 mT), and the presence of a ^{14}N (spin = 1) ligand attached to the lower axial position of the cobalamin results in superhyperfine splitting of each component of the octet into a triplet. Curve B, enzyme isolated from cells grown in glucose minimal M9 medium containing 9.5 mM $^{15}NH_4Cl$ and 2.5 μM ^{14}N-labeled cyanocobalamin. The octet of doublets centered around $g = 2$ indicates that the lower axial ligand for the cobalamin is labeled with ^{15}N (spin = 1/2), and thus derives from the protein rather than the nucleotide loop of the cobalamin. Curve C, enzyme isolated from cells grown in glucose minimal M9 medium containing $^{15}NH_4Cl$, ^{14}N-aquocobalamin and 200 μM ^{14}N-histidine. The reappearance of the octet of triplets indicates that the lower axial ligand is now ^{14}N-labeled. Because exogenous histidine represses de novo histidine biosynthesis from NH_4Cl but does not serve as a nitrogen source for the biosynthesis of other amino acids in the presence of NH_4Cl, this experiment indicates that the lower axial ligand is a nitrogen in a histidyl residue from the protein.

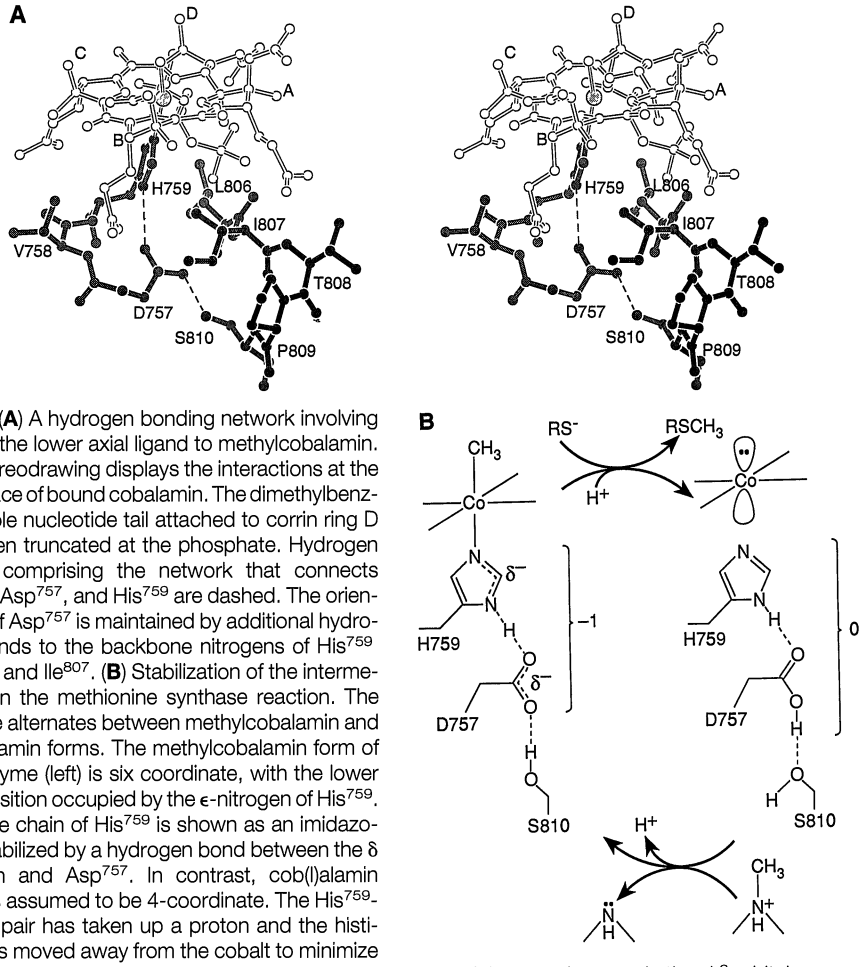

Fig. 8. (**A**) A hydrogen bonding network involving His^{759}, the lower axial ligand to methylcobalamin. The stereodrawing displays the interactions at the lower face of bound cobalamin. The dimethylbenzimidazole nucleotide tail attached to corrin ring D has been truncated at the phosphate. Hydrogen bonds comprising the network that connects Ser^{810}, Asp^{757}, and His^{759} are dashed. The orientation of Asp^{757} is maintained by additional hydrogen bonds to the backbone nitrogens of His^{759} Leu^{806}, and Ile^{807}. (**B**) Stabilization of the intermediates in the methionine synthase reaction. The enzyme alternates between methylcobalamin and cob(I)alamin forms. The methylcobalamin form of the enzyme (left) is six coordinate, with the lower axial position occupied by the ε-nitrogen of His^{759}. The side chain of His^{759} is shown as an imidazolate, stabilized by a hydrogen bond between the δ nitrogen and Asp^{757}. In contrast, cob(I)alamin (right) is assumed to be 4-coordinate. The His^{759}-Asp^{757} pair has taken up a proton and the histidine has moved away from the cobalt to minimize electrostatic repulsion between the imidazole ε-nitrogen and the two electrons in the d_z^2 orbital perpendicular to the corrin of cob(I)alamin. Ser^{810} is hydrogen bonded to Asp^{757}, and may participate in a proton relay that transfers protons from solvent to and from the His^{759}-Asp^{757} pair.

to form a neutral His-Asp pair. Protonation of the His-Asp pair would favor cleavage of the cobalt-methyl bond to form four-coordinate cob(I)alamin. In the second half-reaction, deprotonation of the histidine would increase the nucleophilicity of cob(I)alamin and facilitate attack on CH_3-H_4folate (*23*). The Ser-Asp-His and the cobalt of cobalamin could thus form a catalytic quartet that facilitates methylation and demethylation by ferrying protons in and out of the sequestered region under the cobalt, manipulating the carbon-cobalt bond strength (Fig. 8B). In this mechanism, Ser^{810} provides an essential connection between bulk solvent and the His-Asp pair.

Although Asp^{757} and His^{759} are conserved in the adenosylcobalamin-dependent methylmalonyl-CoA mutases and glutamate mutases, Ser^{810} is only found in the two sequences of methionine synthase. Variations in the hydrogen bonding network below the corrin may account for some of the distinctive properties of cobalamin-dependent enzymes. Methylmalonyl-CoA mutase has been crystallized (*24*). Structural studies of this enzyme and studies of mutant forms of methionine synthase should be invaluable for a detailed understanding of the reactivity of protein-bound cobalamins.

Although the α/β domain of methionine synthase shows no structural similarities to known heme-binding proteins, the corrin and heme macrocycles have many structural and chemical similarities. In cytochrome c peroxidase, which catalyzes the heterolytic cleavage of oxygen bound to the upper axial position of the heme iron, histidine and aspartate residues are located below the heme iron in positions similar to those seen in methionine synthase, even though the protein scaffold for these residues is structurally unrelated (*25*). Reduction of the heme iron of cytochrome c peroxidase from the Fe^{3+} state to the Fe^{2+} state is associated with proton uptake over the pH range from 5 to 8, and disruption of the hydrogen bond between Asp^{235} and His^{175} by mutation of the aspartate profoundly perturbs the pH dependence of the reduction potential and increases its midpoint by 100 mV. It has been suggested that a strong hydrogen bond is formed between Asp^{325} and His^{175}, and that His^{175} is partially deprotonated. Thus convergent evolution may have led to highly similar catalytic motifs in methionine synthase and cytochrome c peroxidase, in response to requirements to modulate the bond strengths of ligands occupying the upper axial positions of their prosthetic groups.

REFERENCES AND NOTES

1. R. L. Blakley, in B_{12}, vol. 2, *Biochemistry and Medicine*, D. Dolphin, Ed. (Wiley, New York, 1982), pp. 381–418; R. Switzer, *ibid.*, pp. 289–305; B. Babior, *ibid.*, pp. 263–287; J. J. Baker and T. C. Stadtman, *ibid.*, pp. 203-232; T. Toraya and S. Fukii, *ibid.*, pp. 233–262; R. T. Taylor, *ibid.*, pp. 307–355; J. Retey, *ibid.*, pp. 357-379; R. G. Matthews, in *Folates and Pterins*, vol. 1, *Chemistry and Biochemistry of Folates*, R. L. Blakley and S. J. Benkovic, Eds. (Wiley, New York, 1984), pp. 497–553.
2. J. Halpern, in B_{12}, vol. 1, *Chemistry*, D. Dolphin, Ed. (Wiley, New York, 1982), pp. 501–541.
3. B. Kräutler, *Helv. Chim. Acta* **70**, 1268 (1987).
4. M. F. Summers *et al.*, *J. Am. Chem. Soc.* **105**, 6259 (1983); M. F. Summers, L. G. Marzilli, N. Bresciani-Pahor, L. Randaccio, *ibid.* **106**, 4478 (1984).
5. D. C. Hodgkin, J. Kamper, M. Mackay, J. Pickworth, *Nature* **178**, 64 (1956); D. C. Hodgkin *et al.*, *Proc. R. Soc. (London)* **A242**, 228 (1957); D. C. Hodgkin *et al.*, *ibid.* **251**, 306 (1959); J. G. White, *ibid.* **A266**, 440 (1962); D. C. Hodgkin, J. Lindsey, M. Mackay, K. N. Trueblood, *ibid.*, p. 475; D. C. Hodgkin, J. Lindsey, R. A. Sparks, K. N. Trueblood, J. G. White, *ibid.*, p. 494; C. Brink-Shoemaker, D. W. J. Cruickshank, D. C. Hodgkin, M. J. Kamper, D. Pilling, *ibid.* **A278**, 1 (1964).
6. P. G. Lenhert and D. C. Hodgkin, *Nature* **192**, 937 (1961); P. G. Lenhert, *Proc. R. Soc. (London)* **A303**, 45 (1968).
7. M. Rossi *et al.*, *J. Am. Chem. Soc.* **107**, 1729 (1985).
8. E. N. G. Marsh and D. E. Holloway, *FEBS Lett.* **310**, 167 (1992).
9. J. T. Drummond, S. Huang, R. M. Blumenthal, R. G. Matthews, *Biochemistry* **32**, 9290 (1993).
10. K. Fujii and F. M. Huennekens, *J. Biol. Chem.* **249**, 6745 (1974); C. Osborne, L.-M. Chen, R. G. Matthews, *J. Bacteriol.* **173**, 1729 (1991); K. Fujii, J. H. Galivan, F. M. Huennekens, *Arch. Biochem. Biophys.* **178**, 662 (1977).
11. R. V. Banerjee, N. L. Johnston, J. K. Sobeski, P. Datta, R. G. Matthews, *J. Biol. Chem.* **264**, 13888 (1989); I. G. Old, D. Margarita, R. E. Glass, I. Saint Girons, *Gene* **87**, 15 (1990); J. T. Drummond, R. R. Orgorzalek Loo, R. G. Matthews, *Biochemistry* **32**, 9282 (1993).
12. C. L. Luschinsky, J. T. Drummond, R. G. Matthews, M. L. Ludwig, *J. Mol. Biol.* **225**, 557 (1992).
13. We thank W. A. Hendrickson for providing the source code for this program, which optimizes the fit of equivalent electron densities related by noncrystallographic symmetry (*39*).
14. A. Brünger, *X-PLOR Version 3.1 Manual* (Yale Univ. Press, New Haven, CT, 1993).
15. C. Cambillau and E. Horjales, *J. Mol. Graphics* **5**, 174 (1987); T. A. Jones and S. Thirup, *EMBO J.* **5**, 819 (1986).
16. M. L. Ludwig and C. L. Luschinsky, in *Chemistry and Biochemistry of Flavoenzymes*, F. Müller, Ed. (CRC Press, Boca Raton, FL, 1992), vol. 3, pp. 427–466; W. Watt, A. Tulinsky, R. P. Swenson, K. D. Watenpaugh, *J. Mol. Biol.* **218**, 195 (1991).
17. G. Eggink, H. Engel, G. Vriend, P. Terpstra, B. Witholt, *J. Mol. Biol.* **212**, 135 (1990); G. E. Schulz, *Curr. Opinion Struct. Biol.* **2**, 61 (1992).
18. N. Kimura and S. Takamuku, *J. Am. Chem. Soc.* **116**, 4087 (1994); D. Lexa, J.-M. Savéant, K.-B. Su, D.-L. Wang, *ibid.* **110**, 7617 (1988).
19. D. Lexa and J.-M. Savéant, *Acct. Chem. Res.* **16**, 235 (1983); M. D. Wirt, I. Sagi, M. R. Chance, *Biophys. J.* **63**, 412 (1992).
20. Methionine synthase selectively stabilizes the cob(I)alamin oxidation state of B_{12}. Cob(II)alamin is much more readily reduced to form cob(I)alamin when the cofactor is bound to the enzyme than when it is free, while reduction of cob(III)alamin to cob(II)alamin is unaffected by binding (*40*).
21. J. A. Tainer, E. D. Getzoff, K. M. Beem, J. S. Richardson, D. C. Richardson, *J. Mol. Biol.* **160**, 181 (1982).
22. J. T. Drummond and R. G. Matthews, *Biochemistry* **33**, 3732 (1994).
23. G. N. Schrauzer and E. Deutsch, *J. Am. Chem. Soc.* **91**, 3341 (1969).
24. N. McKie, N. H. Keep, M. L. Patchett, P. F. Leadlay, *Biochem. J.* **269**, 293 (1990); N. Marsh, P. F. Leadlay, P. R. Evans, *J. Mol. Biol.* **200**, 421 (1988).
25. D. B. Goodin and D. E. McRee, *Biochemistry* **32**, 3313 (1993); D. G. Rousseau and D. L. Rousseau, *J. Structural Biol.* **109**, 13 (1992); T. L. Poulos *et al.*, *J. Biol. Chem.* **255**, 575 (1980).
26. T. C. Terwilliger and D. Eisenberg, *Acta Crystallogr. A* **39**, 813 (1983).
27. Z. Otwinowsky, in *Isomorphous Replacement and Anomalous Scattering*, W. Wolf, P. R. E. Evans, A. G. W. Leslie, Eds. (SERC Daresbury Laboratory, Warrington, UK, 1991), pp. 80–86.
28. W. Steigemann, thesis, Technische Universität, Munich (1974).
29. W. Furey and S. Swaminathan, *Am. Crystallogr. Assoc. Mtg. Abstr.* **18**, 73 (1990).
30. During stages 2 and 3, atoms were selected from the model for use in phase combination according to the appearance of difference Fourier or omit maps. X-PLOR refinements were conducted with noncrystallographic symmetry restraints and included at least 200 cycles of positional refinement before and after simulated annealing from 2000 K. Omit maps of the dimethylbenzimidazole nucleotide side chain indicated a sugar pucker and torsion angles different from those in model cobalamins. Subsequent refinement constrained the cobalamin atoms to the positions that were built into difference maps and were then energy minimized. In these calculations, the folding of the corrin ring system was not permitted to change from that of free methylcobalamin (*7*). Isotropic individual atom temperature factors were refined at the end of stages 2 and 3.
31. R. Read, *Acta Crystallogr. A* **42**, 140 (1986).
32. P. J. Kraulis, *J. Appl. Crystallogr.* **24**, 946 (1991).
33. N. L. Harris, S. R. Presnell, F. E. Cohen, *J. Mol. Biol.* **236**, 1356 (1994).
34. D. R. Smith, GenBank accession number U00017 (1994). Two open reading frames in this cosmid were identified by sequence similarity as metH2 and metH1 and correspond to the 98- and 37-kD domains of metH, respectively.
35. W. Kabsch and C. Sander, *Biopolymers* **22**, 2577 (1983).
36. T. A. Jones, J.-Y. Zou, S. W. Cowan, M. Kjeldgaard, *Acta Crystallogr. A* **47**, 110 (1991).
37. R. Jansen, F. Kalousek, W. A. Fenton, L. E. Rosenberg, F. D. Ledley, *Genomics* **4**, 198 (1989).
38. The EPR data were recorded on a Century Series Varian EPR spectrometer, digitized on a TRACOR-Northern NS-900 Signal Averager and processed with software developed by W. R. Dunham (University of Michigan). The spectra were run with 0.8 mT field modulation and 10 mW microwave power, and these conditions were shown not to result in overmodulation or saturation. Spectra were recorded at 100 K and are the averages of four 8-minute scans.
39. J. M. Cox, *J. Mol. Biol.* **28**, 151 (1967).
40. R. V. Banerjee, S. R. Harder, S. W. Ragsdale, R. G. Matthews, *Biochemistry* **29**, 1129 (1990).
41. Coordinates for the B_{12}-binding domains of methionine synthase have been deposited in the Brookhaven Data Bank (1BMT).

42. Supported by NIH grants GM16429 (M.L.L.) and GM24908 (R.G.M.); by Molecular Biophysics Training Grant GM08570 (C.L.D.); by Pharmacological Sciences Training Grant GM07767 (J.T.D.), and by an NSF Graduate Fellowship (J.T.D.). We thank W. R. Dunham for assistance with the EPR experiment shown in Fig. 7, G. Glick (University of Michigan) for help with the positional refinement of the cobalamin prosthetic group, and F. E. Cohen for an analysis of the helix packing. This article is dedicated to the memory of Dorothy Crowfoot Hodgkin.

1 September 1994; accepted 24 October 1994